Polym. Bull. (2009) 62:391–403
DOI 10.1007/s00289-008-0015-x

ORIGINAL PAPER

Effect of processing conditions on the structural morphology of PP–EP/EVA/organoclay ternary nanocomposites

E. Ramírez-Vargas · M. Valera-Zaragoza · S. Sánchez-Valdes · J. S. Hernández-Valdez · F. F. Ibarra-Castillo

Received: 9 July 2007 / Revised: 19 May 2008 / Accepted: 23 November 2008 /
Published online: 5 December 2008

Abstract The effect of processing conditions on the morphology of heterophasic PP–EP/EVA/organoclay ternary nanocomposites was examined. The nanocomposites were prepared in a co-rotating twin screw extruder with different screw configurations and incorporation methods. Three different sizes of EVA granules were used. The results obtained by X-ray scattering (WAXD) and electronic microscopy (TEM) showed an increase in *d* spacing value of the clay associated with the polar interactions between the vinyl acetate of EVA and the surface of the nanoclays. In addition, some chains of the non-polar copolymer PP–EP may have become intercalated into the clay galleries as a result of polymer diffusion induced by shear stress during melt mixing. An increase in surface area of EVA granules resulted in a more homogenous clay dispersion and intercalation. The morphologic changes resulted in an increase in heat distortion temperature (HDT) and flexural modulus of the ternary nanocomposites.

Keywords Nanocomposites · Nanoclays · Processing · Polypropylene · EVA

Introduction

Polymer–clay nanocomposites have received special attention because of their improved properties at very low loading levels compared with conventional filler

E. Ramírez-Vargas (✉) · M. Valera-Zaragoza · S. Sánchez-Valdes · J. S. Hernández-Valdez · F. F. Ibarra-Castillo
Centro de Investigación en Química Aplicada (CIQA),
P.O. Box 379, Saltillo, Coahuila 25253, Mexico
e-mail: evargas@ciqa.mx

S. Sánchez-Valdes
e-mail: saul@ciqa.mx

composites. It is well known that the enhancement in properties is related to a homogeneous dispersion and exfoliation of the organoclay into the polymer matrix, however the dispersion depends on several factors, such as the polymer polar groups [1, 2] and the structural characteristics of the clay modifier [3, 4]. However, the diffusion of polymer chains into the clay galleries during melt processing has an important role in the dispersion of the clay galleries. Dennis et al. [5] observed differences in the morphology of nylon 6/clay nanocomposites when using extruders with different screw configurations. They found that high and low shear configurations did not affect significantly the clay dispersion suggesting that a balance in shear has an important effect on the polymer diffusion between intergallery spacing of the clay. It has been previously proved that polymer diffusion and intergallery interactions have a major influence on the exfoliation in polymer–clay nanocomposites. It has been reported that in binary nanocomposite systems with polar polymers, the clay galleries are dispersed directly into the polymer matrix, affecting only the polymer–clay interactions, such as interactions between the polar domains of the polymer and that of the nanoclay surface [6]. In the case of non-polar polymers such as polypropylene [7–10] and polyethylene [11, 12], a compatibilizing agent between the organic and inorganic phases has been used, such as oligomers of PP grafted with maleic anhydride. In these systems, it has been important to study the compatibilizer–clay [8, 9] and compatibilizer–polymer [10] interactions. Even though these systems involve three components they can not be defined as ternary nanocomposites because of the composition and the different molecular weight of the polymers. In a ternary system, in which two of the components are polymers and one is clay, different factors influence the final morphology of the nanocomposite, such as the concentration of each component, compatibility between polymers and interaction of the clay with one or both polymers during melt mixing. It is possible that the method of incorporation of the three different polarity components into the extruder may affect the intrinsic molecular interactions of the system and, consequently, the final material performance. Some studies on the morphology of ternary nanocomposites have been reported. Chow et al. [13, 14] studied PA6/PP/organoclay nanocomposites determining the interaction between clay galleries on the system. The results of these works have been focused on the morphologic changes in the system as a result of intermolecular interactions. On the other hand Li et al. [15] studied the influence of the sequence of mixing on the microstructure of ternary PBT/EVA/clay. These authors report significant differences in the morphology of the nanocomposites, observing higher dispersion of the nanogalleries into the polymer matrix, when the PBT and clay are premixed in a first step, followed by mixing with EVA in a second step. They explained this behavior by considering the interfacial interactions between hydroxyl groups on the clay with PBT matrix. In these previously reported works [16], each ternary system exhibited morphologies that depended on the components and the preparation conditions. The main purpose of this work is to study the nano structure of the ternary system PP–EP/EVA/organoclay, under different processing conditions and its effect on the final properties of the nanocomposites.

Experimental

Materials

A heterophasic polypropylene–(ethylene-propylene) (PP–EP) copolymer with an ethylene content of 8 wt% from Montell Polyolefins Inc. was used. An ethylene vinyl acetate (EVA) copolymer with vinyl acetate (VA) content of 18 wt% was supplied by Du Pont Inc. Cloisite 20A, an organically modified nanoclay with dimethyl dihydrogenated tallow quaternary ammonium chloride (two hydrogenated tallows), was supplied by Southern Clay, Inc.

Preparation of nanocomposites

A Werner and Pfleiderer co-rotating twin screw extruder (model ZSK-30) was used to obtain the nanocomposites. The content of organoclay Cloisite 20A was 6 wt% with respect to the EVA copolymer and 2.4 wt% with respect to the PP–EP/EVA/organoclay ternary system. The EVA content was 40 wt%. The studied variables were as follows:

Incorporation sequence Four incorporation sequences were studied by changing the order in feeding of the three components to the extruder. Table 1 shows the description of the sequences used. S1 indicates the mixing of the three components (PP–EP/EVA/nanoclay) at the same time and melting them in a one-step mixing at a temperature above the melting temperature of PP–EP. S2 indicates the incorporation of PP–EP/EVA polymer system in a first step in order to obtain a polyolefin blend with adequate compatibility as was previously reported [17], and in a second step incorporate the organoclay trying to maintain the compatibility characteristics in the polyolefin blend. S3 is a melt combination of PP–EP with nanoclay followed by the incorporation of EVA in a second step. S4 indicates the melt mixing of EVA with clay and the obtained compound is then mixed again with the PP–EP obtaining a ternary nanocomposite.

EVA granule size Three different granule sizes were examined. One was the pellet as it was received, the others were obtained from the milling of the original pellet using a blade ultracentrifuge miller (RETSH ZM100) until different mesh

Table 1 Incorporation methods and steps of mixing

Sample	Nanocomposite	Step of mixing	Components
S1	PP–EP/EVA/C20A	1°	PP–EP + EVA + C20A
S2	(PP–EP/EVA)/C20A	1°	PP–EP + EVA
		2°	PP–EP/EVA + C20A
S3	(PP–EP/C20A)/EVA	1°	PP–EP + C20A
		2°	PP–EP/C20A + EVA
S4	(EVA/C20A)/PP–EP	1°	EVA + C20A
		2°	EVA/C20A + PP–EP

sizes was obtained. The volumes of the considered granules, measured by optical microscopy with image analyzer, were 1.76, 9.22, and 44.16 cm^3. Each granule size was mixed with the nanoclay using the sequence described in S4.

Screw configuration Three mixing screw configurations were used. The level of shear in each screw configuration was changed by modifying the number of kneading elements and the reverse conveying elements and denoted as low (1), medium (2), and high (3) shear configurations. In this way, the obtained nanocomposites using each screw configuration were designated with the respective number indicating the screw configuration used. This study considered the nanocomposites obtained from the incorporation sequence S4. Residence time was measured by adding a tracer (coloured pellet) into the feed hoper taking the initial time (t_i) and final time (t_f) as the first and last pigmented polymer melt was obtained through the output of the extruder. The average residence time was calculated by $(t_i + t_f)/2$.

Melt temperature The EVA-clay melt mixing temperatures considered were: 130, 150 and 170 °C based on the incorporation sequence S4.

Evaluation of nanocomposites

Ultra-thin sections of nanocomposites with 1 mm^2 of area and an average thickness of 70 nm were obtained using an Ultracut Leica EMFCS ultra microtome, equipped with diamond knife, and liquid nitrogen. Transmission electron microscopy images were obtained from these specimens, using a Jeol 1200-EXII transmission electron microscope with an acceleration voltage of 60 kV. At least five samples from bars for mechanical tests of each nanocomposite were prepared for TEM analysis, scanning different fields of each sample. The shown TEM images are the representative images of each sample. Negatives were scanned in a Duoscan T2500 AGFA scanner using the Fotolook 32 V3.60.0 software from Adobe Photoshop. X-Ray diffraction patterns were obtained in a Siemens D-500 diffractometer using a Ni-filtered CuK-alpha radiation generator with an intensity of 25 mA and an accelerating voltage of 35 kV. The diffraction patterns were collected within the 2θ range 0.5–40° using a scanning rate of 0.6°/min. The d spacing was calculated according to Bragg's equation. The rheological behaviour was measured at 200 °C with a capillary rheometer (Instron 4467), using a die with an L/D of 27.55. Flexural modulus was measured according to ASTM D 882 with an Instron Model 4301. Heat distortion temperature (HDT) was measured according to ASTM D-648.

Results and discussion

Effect of the incorporation method on the morphology

Figure 1a presents the comparative X-ray diffraction patterns for the four previously described (Table 1) incorporation methods; S1, S2, S3 and S4. All the diffraction patterns show the characteristic peaks of an intercalated morphology. The peaks

related to the layer expansion associated with the intercalated structures at $2\theta = 2.32$ do not show a change in the angle value among them, indicating that the average interlayer spacing remains unchanged, with any of the incorporation methods used. However, the diffraction peak intensity between the methods is quite different. It has been reported that the intensity and broadening of the peak related to interlayer spacing is indicative of an intercalated structure. If the diffraction peak has higher intensity and less broadening (more defined signal), more ordered intercalated layer structures have been obtained. On the other hand, if the peak has less intensity and more broadening (less defined signal) more disordered intercalated layer structures have been obtained [18], which are closer to an exfoliated structure. In our case, it can be seen that the diffraction peak intensity is lower for S4, which suggests that with these methods a more disordered intercalated structure than the other incorporation sequences, has been obtained. This could be related to the fast interaction between VA of EVA and the organoclay polar surface. It has been reported [19] that particle exfoliation or intercalation is related with specific interactions between the polar groups in the polymer matrix and the polar organically-modified surface of clay layers. In this particular case, the polar VA groups of the EVA matrix can interact with the modified surface of the clay. In addition, OH groups present on the unmodified side areas of clay might also be able to interact with the polar groups of EVA matrix.

S1 and S2 show a similar behaviors and S3 shows a more defined peak with higher intensity, indicating the formation of an intercalated-ordered morphology. This EVA-clay interaction remains even when the PP–EP is incorporated in a second step according to method S4. On the other hand, if the initial mixing is between PP–EP and clay, only a few polymer PP–EP chains are intercalated into the clay galleries mainly because of the polymer viscosity and the shear stresses involved during melt mixing. The result is a morphology with a low intercalation structure as is shown in Fig. 1b, where the spacing of the layer clays of the PP–EP/C20A hybrid is lower than when EVA is included in the ternary system (S3). The lack of polar groups in PP–EP is an important factor that inhibits favorable polymer–clay interactions. However, an inter gallery spacing of 95 nm of PP–EP/

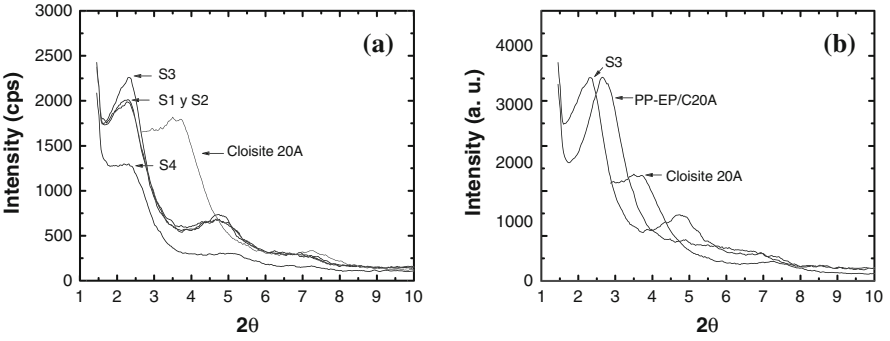

Fig. 1 X-ray diffraction patterns for C20A and PP–EP/EVA/Clay nanocomposites prepared by different methods: **a** S1, S2, S3 and S4 and **b** incorporation method S3

C20A compared with the neat C20A organoclay suggests that the shear stresses induced by the mixing elements of the twin screw extruder may have an influence on the clay aggregates separation, forming tactoids and allowing the diffusion of some polymer chains into the clay galleries without a complete layer separation, even though the polymer chains interact weakly with the clay surface.

Since the X-ray diffraction patterns are an average of the repetitive crystallographic planes of the nanoclay, it is possible to identify an intercalated layer structure by this technique. However, TEM is necessary to clearly define an exfoliated structure. In a previous work [16] we reported intercalated–exfoliated morphologies for this ternary nanocomposite prepared by only one incorporation method. Figure 2a exhibits the morphology for the incorporation method S4, where mainly intercalated layers can be observed as well as some exfoliated clay layers into the polymer matrix, resulting in an intercalated–exfoliated morphology. The fact that the clay layers are partially exfoliated, indicates favorable polar interactions between VA groups of EVA and the clay polar surface. These interactions have been widely described in a previous work [20]. On the other hand, when the non-polar heterophasic PP–EP polymer is combined with the organoclay in a first extrusion step, an intercalation mechanism occurs originated only by the polymer diffusion through inter gallery spacing, where the organoclay galleries, previously separated by the polar modifier, are separated even more by the particular shear stresses of the twin screw extruder during melt mixing. This diffusion mechanism may preferably form a tactoidal morphology. Figure 2b, shows the incorporation method S3, in which, even though there are some tactoids attributed to a lower intercalation degree, it is possible to see some clay layers dispersed into the polymer matrix as a result of the EVA/clay interactions during the second step of mixing. This suggests that the clay separation may have originated by the polymer melt diffusion caused by the shear stress and the polar interaction between VA and clay surfaces. Considering the obtained results it is preferable to incorporate EVA polymer with the organoclay in a first step in order to enhance the favorable interactions between them and then, in a second step, incorporate the

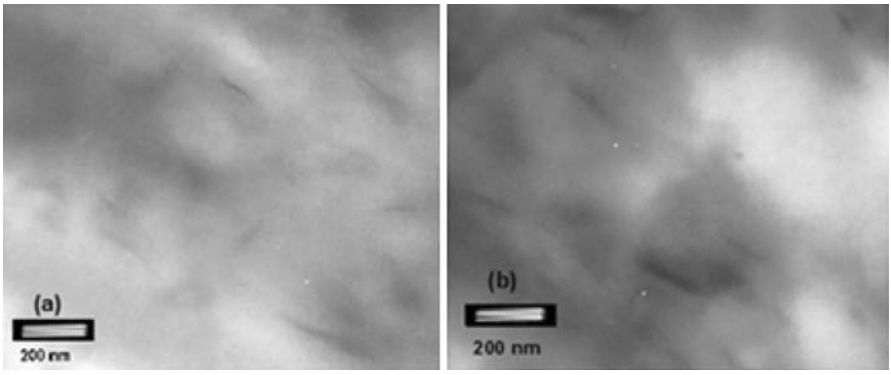

Fig. 2 TEM images of nanocomposites samples: **a** (EVA/C20A + PP–EP) prepared by S4 and **b** (PP–EP/C20A + EVA) prepared by S3

PP–EP to the hybrid melting (method S4). The incorporation method S1, is also recommendable, but the PP–EP may interfere in the EVA-clay interactions.

Effect of the EVA granular size

The materials used for the nanocomposites preparation were of different granule size, the polymers used were granules with an average size of 3–5 mm and the organoclays were dust particles with an average diameter of 0.1 mm. In order to increase the surface area of the polymer granules and enhance the interactions with the organoclay, the incorporation of EVA polymer with different granule sizes was studied. Figure 3 shows the intergallery spacing as a function of the reduction in EVA granule volume. It can be seen that the interlayer spacing is increased as the granule volume is reduced. This suggests that the milling of the EVA pellets would increase their surface area and enhance the mixing possibilities between the clay particles during the preparation of the formulation previous to the melt mixing, and as a consequence a better clay particle dispersion in the EVA matrix during melt mixing can be achieved. This enhanced dispersion increases the breaking of clay aggregates and increase the possibility of polymer diffusion in to the clay galleries and as a result a higher degree of intercalation can be achieved (Fig. 4). The morphology is maintained even after the PP–EP is incorporated to obtain the ternary complex. In a previous work [20], we have confirmed that the structural morphology obtained for the hybrid EVA/C20A is maintained in the PP–EP/(EVA/C20A) ternary system, in which the clay layers are located in the EVA phase. The results indicate that once the EVA is attached to the clay surface, the system remains stable, allowing nanocomposite materials with improved final properties to be prepared. Additionally, the compatibility between the PP–EP and EVA blend, as was described in previous reports [17], was not affected by the incorporation of the clay.

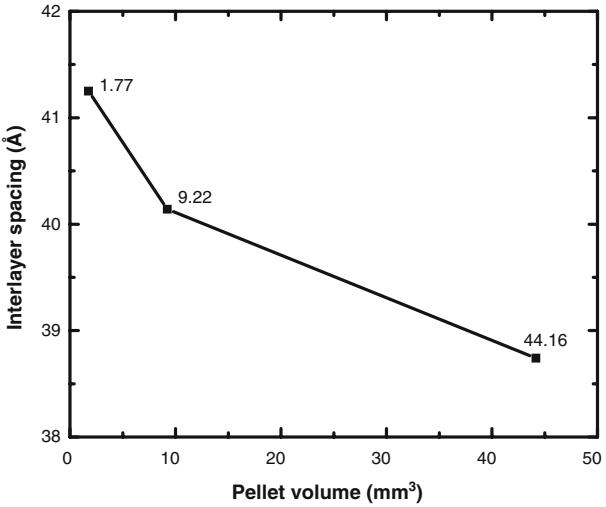

Fig. 3 Interlayer spacing versus EVA pellet volume for the PP–EP/EVA/C20A ternary system

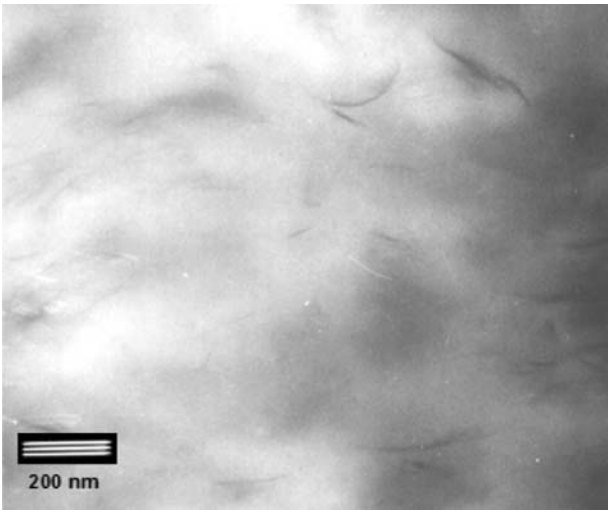

Fig. 4 TEM image of EVA/C20A nanocomposite with lower EVA pellet size

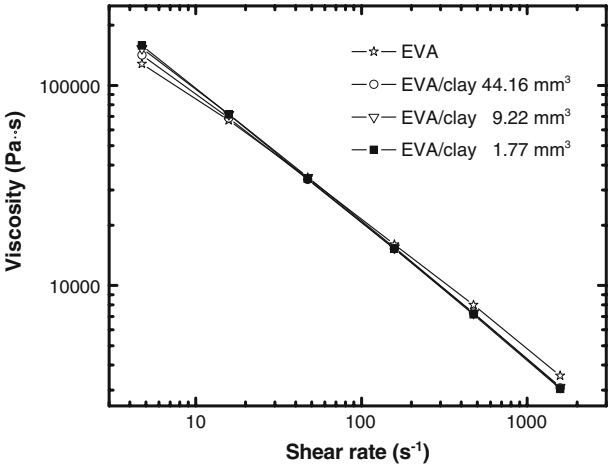

Fig. 5 Shear viscosity for EVA/C20A nanocomposite with different EVA pellet volume

Figure 5 shows the comparative results of apparent viscosity for the EVA/C20A system with the three studied granule volumes. It can be seen that the effect of granule volume on shear viscosity is almost imperceptible. However, it can be seen that at higher EVA granule volume lower shear viscosity is obtained. This could be related to the less homogeneous clay distribution obtained when using the higher EVA granule volume, in which lower interactions between EVA and clay could be achieved, as was discussed in XRD results. Regions with higher EVA and less clay content could be obtained and this could reduce the shear viscosity. It can also be seen that at low shear rates all the polymer nanocomposites show higher melt

viscosities than the raw polymer while at high shear rates the melt viscosity of the nanocomposites is reduced. This could be explained that at low shear rates, the clay layers are only partially separated and random oriented, which increases the melt viscosity. In contrast, at higher shear rates, the clay layers are strongly orientated toward the flow direction which would reduce the melt viscosity. This result is in agreement with the results obtained by other authors [21, 22].

Effect of screw configuration and melt temperature

The shear stresses during melt processing enhance the PP–EP chain diffusion into the clay galleries even though there are no polar polymer–clay interactions. If the macromolecular diffusion increases the polymer–clay intercalation, so the number of shear screw elements and their distribution through the screw may influence the breaking of clay aggregates facilitating the entrance of polymer chains during melt processing. Even though there is not necessarily a direct relation between the increase in shear stress and the clay exfoliation [23]. Taking this into consideration, different screw configurations were studied. The twin screw extruder used has a flexible screw configuration with intermeshing screw elements that can be assembled into conveying (forward and reverse) and kneading (forward and reverse) elements. The forward conveying elements are simply for producing the forward flow of the melt, which at the same time tends to increase the pressure at the front. The reverse conveying elements tend to produce a backwards flow of the melt, resulting in a reduced flow in the forward direction, allowing for the melt to remain for an extended residence time in the sections immediately before the reverse conveying element. Meanwhile the forward kneading elements are designed in a variety of lengths and pitches and have the same direction as the forward conveying elements. These forward kneading elements tend to predominantly produce the dispersive mixing. The reverse kneading elements are also designed in a variety of lengths and pitches and have the same direction as the reverse conveying elements. These reverse kneading elements tend to predominantly produce the distributive mixing and increase residence time. The low shear intensity screw configuration (Fig. 6a) had only two forward conveying blocks early in the screw to melt the resin, meanwhile the medium shear screw (Fig. 6b) was designed with a standard compression ratio and rarely include reverse conveying elements. These are used both for melting and compounding tasks. The high shear screw (Fig. 6c) incorporate elements which generate high shear in order to improve the dispersion behavior. In the case of a co-rotating screw, this is achieved through the application of kneading and reverse conveying elements. This design would increase the time during which the material is subjected to the high shear of the kneading elements, which would break the particle aggregates and increase their dispersion through the polymer matrix. Residence times for each configuration were determined; for low shear a residence time of 77 s was obtained and for medium and high shear 93 and 96 s, respectively were obtained.

It is apparent that even when the shear stress influences the polymer chain diffusion into the inter-gallery spacing, this is not the key factor in obtaining highly exfoliated morphologies, since the exfoliation rate is mainly dependent on the polar

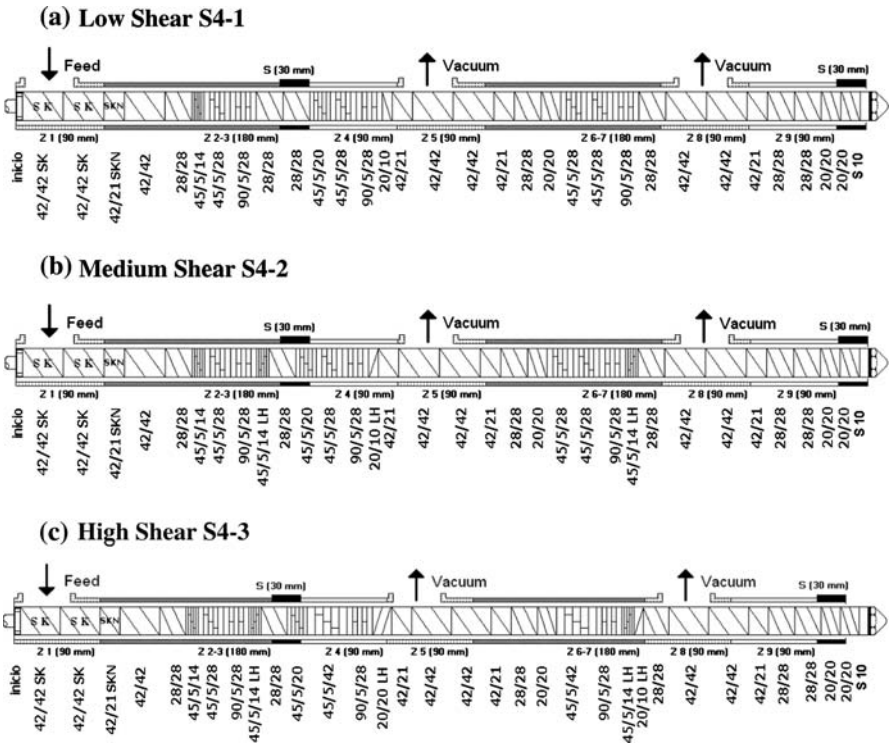

Fig. 6 Screw configurations used in the twin screw extruder

interactions between polymer and clay. Once a maximum intercalation or intercalation–exfoliation is reached, it is difficult to exceed it by increasing the shear stress. It is reported that higher residence times improve the dispersion exfoliation process; however this exfoliation is difficult to extend by increasing the shear stress. Dennis et al. [5] has reported that stacks of platelets are decreased in height at high shear intensities. The process of the polymer entering the clay galleries does not require high shear intensity but involves diffusion of polymer into the clay galleries driven by chemical affinity and facilitated by residence time in the extruder. Considering this, and observing Fig. 7a, the medium shear configuration, which has a mean residence time of 93 s, quite similar to that obtained for the high shear configuration (96 s), offers an adequate shear to obtain an intercalated–exfoliated structure. On the other hand the high shear configurations reduced the HDT and flexural modulus. This is in agreement with the works reported [5] in which the high shear stress reduces the exfoliation rate. The other studied processing variable was the melt temperature. The temperature profiles tested were 130, 150 and 170 °C. The X-ray diffraction patterns shown in Fig. 7b, indicate that the layer expansion reaches a maximum at 150 °C, and above this temperature it is reduced. This result suggests that the system melt viscosity is reduced at higher temperatures inhibiting the complete separation of the clay aggregates or tactoids. In

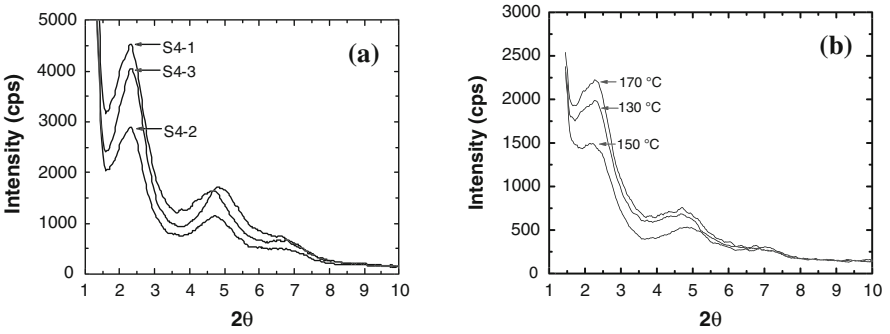

Fig. 7 X-ray diffraction patterns for **a** different screw configurations: S4-1, S4-2 and S4-3 and **b** (EVA/C20A)/PP–EP nanocomposites at 130, 150 and 170 °C melt temperatures

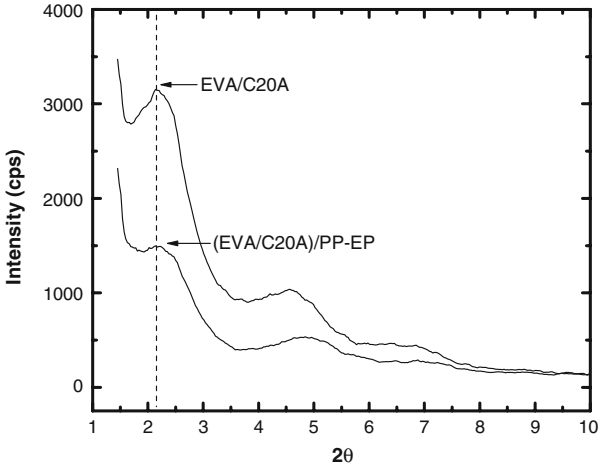

Fig. 8 X-ray diffraction patterns for EVA/C20A and PP–EP/EVA/C20A at 150 °C melt temperature

order to obtain higher interactions between EVA polymer chains and clay layers it is necessary to apply sufficient shear stress and high melt viscosity capable to achieve an adequate tactoid stacking dispersion. Once the morphology was established for the hybrid EVA/C20A, it remained during the melt mixing with the PP–EP even under the melting conditions used for the PP–EP as it shown in Fig. 8.

Final properties

The morphology results are reflected on the nanocomposite final properties as shown in Table 2. One of the properties that is strongly affected is the HDT. An increase in the HDT is related to the reinforcement of the clay and the amount of intercalation reached between the different systems. The same behaviour is seen on flexural modulus.

Table 2 Flexural modulus and heat deflection temperature for the studied nanocomposites

Sample	Flexural modulus (psi)	HDT (°C)
PP–EP/EVA	81040	–
S1	89106	45.9
S2	85420	45.6
S3	81691	45.1
S4	88499	46.3
S4-1.77	92479	44.7
S4-9.22	91336	45.1
S4-44.16	89379	42.9
S4-130	88499	46.3
S4-150	83063	44.7
S4-170	85725	44.7
S4-1	88560	43.1
S4-2	89379	42.9
S4-3	83501	42.7

Conclusions

The degree of intercalation in the PP–EP/EVA/C20A system mainly depends on the polymer-clay polar interactions, particularly the interactions between acetate groups of EVA and the surface of nanoclays. The incorporation order of the components has an effect on the intercalation process. The best results were obtained by mixing in a first step, the EVA polymer with C20A clay and then incorporating the obtained hybrid with the PP–EP polymer, in a second mixing step. Although the PP–EP is a non polar polymer, it is possible to diffuse some polymer chains into the clay galleries through the diffusion of polymer melt. The initial clay dispersion depends on the surface contacts of the EVA granules, since with a lower volume in the EVA granules a better dispersion was achieved, enhancing the breaking of the clay agglomerates and tactoids during the melt processing and increasing the intercalation. Even though high shear stresses have a favourable effect on the polymer diffusion through the interlayer spacing, higher shear stresses may collapse an intercalated morphology in to a tactoidal morphology, as was observed in the TEM, and thus reduce mechanical properties. The shear viscosity obtained at temperatures lower then 150 °C had a favorable effect on the formation of intercalated structures.

Acknowledgments The authors wish to thank the Mexican National Council for Science and Technology (CONACYT) for its financial support to carry out this study through project SEP-2006-P49143-Y. Finally, the authors wish to thank to Concepcion-Gonzalez, Josefina-Zamora, Blanca-Huerta, Miriam-Lozano, Mario-Palacios and Jesuz-Rodriguez.

References

1. Fornes TD, Yoon PJ, Hunter DL, Keskkula H, Paul DR (2002) Effect of organoclay structure on nylon 6 nanocomposite morphology and properties. Polymer 43:5915

2. Fornes TD, Paul DR (2004) Structure and properties of nanocomposites based on nylon-11 and -12 compared with those based on nylon-6. Macromolecules 37:7698
3. Lan T, Kaviratna PD, Pinnavaia TJ (1995) Mechanism of clay tactoid exfoliation in epoxy-clay nanocomposites. Chem Mater 7:2144
4. Fornes TD, Hunter DL, Paul DR (2004) Nylon-6 nanocomposites from alkylammonium-modified clay: the role of alkyl tails on exfoliation. Macromolecules 37:1793
5. Dennis HR, Hunter DL, Chang D, Kim S, White JL, Cho JW, Paul DR (2001) Effect of melt processing conditions on the extent of exfoliation in organoclay based nanocomposites. Polymer 42:9513
6. Borse NK, Kamal MR (2006) Melt processing effect on the structure and mechanical properties of PA-6/nanocomposites. Polym Eng Sci 46:1094
7. Hasegawa N, Kawasumi M, Kato M, Usuki A, Okada A (1998) Preparation and mechanical properties of polypropylene–clay hybrids using a maleic anhydride-modified polypropylene oligomer. J Appl Polym Sci 67:87
8. García LD, Picazo O, Merino JC, Pastor JM (2003) Polypropylene–clay nanocomposites: effect of compatibilizing agents on clay dispersion. Eur Polym J 39:945
9. Hasegawa N, Usuki A (2004) Silicate layer exfoliation in polyolefin/clay nanocomposites based on maleic anhydride modified polyolefins and organophilic clay. J Appl Polym Sci 93:464
10. Kawasumi M, Hasegawa N, Kato M, Usuki A, Okada A (1997) Preparation and mechanical properties of polypropylene–clay hybrids. Macromolecules 30:6333
11. Zhai H, Xu W, Guo H, Zhou Z, Shen S, Song Q (2004) Preparation and characterization of PE and PE-g-MAH/montmorillonite nanocomposites. Eur Polym J 40:2539
12. Koo CM, Ham HT, Kim SO, Wang KH, Chung IJ, Kim DC, Zin WC (2002) Morphology evolution and anisotropic phase formation of the maleated polyethylene-layered silicate nanocomposites. Macromolecules 35:5116
13. Chow WS, Mohd Ishak ZA, Ishiaku US, Krger-Kocsis J, Apostolov AA (2004) The effect of organoclay on the mechanical properties and morphology of injection-molded polyamide 6/polypropylene nanocomposites. J Appl Polym Sci 91:175
14. Chow WS, Abu Bakar A, Mohd Ishak ZA, Karger-Kocsis J, Ishiaku US (2005) Effect of maleic anhydride-grafted ethylene–propylene rubber on the mechanical, rheological and morphological properties of organoclay reinforced polyamide 6/polypropylene nanocomposites. Eur Polym J 41:687
15. Li X, Park HM, Lee JD, Ha CS (2002) Effect of blending sequence on the microstructure and properties of PBT/EVA-g-MAH/organoclay ternary nanocomposites. Polym Eng Sci 42:2156
16. Valera ZM, Ramírez VE, Medellín RFJ, Huerta MB (2006) Thermal stability and flammability properties of heterophasic PPEP/EVA/organoclay nanocomposites. Polym Degrad Stab 91:1319
17. Ramírez VE, Medellín RFJ, Navarro RD, Avila OC, Solís RS, Lin JS (2002) Morphological and mechanical properties of polypropylene [PP]/poly(ethylene vinyl acetate) [EVA] blends. II. Polypropylene–(ethylene–propylene) heterofasic copolymer [PP–EP]/EVA systems. Polym Eng Sci 42:1350
18. Vaia RA, Giannelis EP (1997) Polymer melt intercalation in organically-modified layered silicates: model predictions and experiment. Macromolecules 30:8000
19. Dumont MJ, Valencia AR, Emond JP, Bousmina M (2007) Barrier properties of polypropylene/organoclay nanocomposites. J Appl Polym Sci 103:618
20. Valera ZM, Ramírez VE, Medellín RFJ (2008) Preparation and morphological evolution of heterophasic PP–EP/EVA/organoclay nanocomposites. Effect of the nanoclay organic modifier. J Appl Polym Sci 108:1986
21. Boucard S, Duchet J, Gerard JF, Prele P, Gonzalez S (2003) Processing of polypropylene–clay hybrids. Macromol Symp 194:241
22. Chow WS, Mohd Ishak ZA, Karger-Kocsis J (2005) Morphological and rheological properties of polyamide 6/poly(propylene)/organoclay nanocomposites. Macromol Mater Eng 290:122
23. Yang K, Ozisik R (2006) Effect of processing parameters on the preparation of nylon 6 nanocomposites. Polymer 47:2849